Solid sorbents for gaseous iodine capture and their conversion into stable waste forms

R. Pénélope, L. Campayo, M. Fournier, A. Gossard, A. Grandjean

Solid sorbents for gaseous iodine capture and their conversion into stable waste forms

R. Pénélope[1], L. Campayo[1], M. Fournier[1], A. Gossard[2], A. Grandjean[2]

[1] CEA, DES, ISEC, DE2D, University of Montpellier, Marcoule, F-30207 Bagnols sur Cèze, France

[2] CEA, DES, ISEC, DMRC, University of Montpellier, Marcoule, F-30207 Bagnols sur Cèze, France

raphael.penelope@cea.fr

CEA Marcoule, ISEC/DE2D/SEVT, Bât. 208, BP17171, 30207 Bagnols-sur-Cèze Cedex, France

Abstract

The reprocessing of nuclear fuel generates gaseous radionuclides including various isotopes of xenon, krypton and iodine. Iodine, mainly present as long-lived ^{129}I (half-life, 1.57×10^7 years) and short-lived ^{131}I (half-life, 8.02 days) is a particular concern because of its high volatility and mobility in the environment. Deep geological disposal is therefore favored over release into the marine environment or the atmosphere. To this end, gaseous iodine must first be captured in solid sorbents and then immobilized in a stable waste form. While the literature on iodine sorbents (also called filters) and iodine immobilization materials is extensive, the conversion of the sorbents into stable waste forms has not received as much attention. The aim of this review is to examine the links between these two research fields: iodine trapping on solid sorbents and iodine conditioning matrices described in the literature.

Keywords: adsorption, disposal, environment, filter, immobilization, nuclear, matrix

1.

2. Introduction

Nuclear fuel reprocessing generates various types of waste, notably minor actinides and fission products. These are managed using different treatment processes depending on their level of activity and half-life. High-level waste is more often vitrified for deep geological disposal [1–4]. One of the main isotopes of iodine in fission products is iodine-131, whose short half-life (8.02 days) and high radioactivity (4.6×10^{15} Bq·g^{-1}) make it particular dangerous if released into the environment [5–7]. The other main iodine isotope produced by fission, iodine-129 (6.7×10^{6} Bq·g^{-1}) poses a long-term risk because of its long radioactive half-life (15.7 million years) [5–7]. As well as being highly volatile and propagating readily in air and groundwater, iodine is absorbed by the thyroid gland in mammals, and exposure to high doses therefore has severe toxic effects [8,9].

This means that specific processes are required to manage radioactive iodine. Vitrification in borosilicate glass, as used for high-level waste, is not a viable option since iodine volatilizes rapidly at the high temperatures involved (> 1000°C) [10–12]. As a result, iodine is managed in some countries such as France and the UK by isotopic dilution in marine environments limited by reject regulations.

Other management approaches that avoid release into the environment are under study. Transmutation, which involves transforming long-life radionuclides into shorter-lived radioisotopes or stable elements, is an attractive solution [13–16]. However, deep geological disposal is currently seen as the most feasible alternative.

48 This approach rests on the immobilization of iodine in a durable matrix material guaranteed to
49 remain stable over millions of years in the chosen geological environment. Different materials
50 have been studied for this application with most of the studies focused on ceramics and
51 glasses [17]. For instance, in the French context, for ceramics, apatites with several
52 compositions (lead-vanadate, calcium-phosphate …) have received much attention [18–20]
53 because of their irradiation stability and high iodine content [21]. This interest comes from
54 geological investigations of the natural nuclear reactors in the Franceville basin (Gabon) that
55 have shown that they have good long-term durability [22,23]. For glasses, low temperature
56 forming glasses are often required to overcome volatility issues coming from the poor thermal
57 stability of iodine-containing materials. This feature can be illustrated by the case of silver
58 phosphate-based glasses [24–26] that have low melting temperature and can incorporate high
59 iodine amount [27].
60 Before immobilization however, the gaseous iodine produced in nuclear fuel reprocessing
61 plants needs to be captured efficiently. This can be done using various wet processes (caustic
62 scrubbing, the Iodox or Mercurex processes [28–32]) or by dry scrubbing, using solid
63 sorbents. The main advantage of dry systems is that non-dispersible solid waste is obtained
64 directly compared to wet processes where several steps are required. Selective solid sorbents
65 for iodine capture have been reviewed extensively [17,33–35], but the question of
66 transforming these materials into a stable waste form is rarely discussed. When it is discussed,
67 several steps are often necessary to get a suitable wasteform from a solid sorbent designed for
68 the trapping of gaseous iodine and this requires most of the time the use of chemical processes
69 [17]. Actually, very few solid sorbents were seen “versatile” enough to be directly converted
70 in a minimum of steps into a dense monolith that could be further disposed of in a deep
71 geological repository. However, new insights have been obtained in this field in the recent

years and it was thought that it could be a good opportunity to make a freeze on the current state of the art in this field.

Hence, the aim of this review is to investigate the possible links between the selective iodine sorbents described in the literature and the immobilization matrices (monolithisation processes) that have been developed from these sorbents.

The first part of the review focuses on the various mechanisms available to capture molecular (I_2) and organic (CH_3I) iodine. Then, the iodine trapping properties of sorbents from literature is presented according to their composition. Their direct transformation (processes in which sorbents are used directly as a primary material without prior transformation) into waste forms after iodine capture is also discussed. The physicochemical properties (microstructure, chemical durability etc.) of the resulting waste forms are discussed in detail. Sorbents whose conversion into waste forms has not be studied or involves wet processing and potential secondary iodine effluents are not considered.

3. Iodine capture mechanisms

Various sorbents can be used to capture molecular or organic gaseous iodine through several mechanisms. In physisorption, iodine is captured on the surface of the sorbent via weak and readily reversible Van der Waals-type interactions. This is the phenomenon typically exploited in metal-organic frameworks (MOFs) [36–38] and activated carbon [39–41]. In other sorbents, the reactivity of certain metals and cations for iodine is exploited to capture the latter by chemisorption in what are known as the active sites of the sorbent. On interaction with these active sites, gaseous iodine forms salts, mainly iodide (I^-) compounds. Iodine is then captured irreversibly through the formation of strong chemical bonds with high dissociation energies. Different chemical reactions can occur depending on the nature of

active site (metallic, cationic) and the type of iodine (molecular or organic) involved. Molecular iodine reacts with metallic active sites (a metallic element, M) as follows:

$$M^0_{(s)} + (a/2)I_{2(g)} \rightarrow MI_{a(s)} \quad (1)$$

(a is an integer greater than 0).

The reaction with organic iodine is similar, but with hydrocarbons as secondary products:

$$M^0_{(s)} + aCH_3I_{(g)} \rightarrow MI_{a(s)} + \text{hydrocarbons}_{(g)} \quad (2)$$

When the active site is cationic (M^{a+}) and integrated in the sorbent's structure (rather than forming a separate phase), this means it contributes to the electrical neutrality of the material. Reactions with iodine thereby lead to a charge deficit. With organic iodine, the reaction can be charge balanced by positively charged methyl groups:

$$xM^{a+}_{(s)} + yCH_3I_{(g)} \rightarrow xMI_{a(s)} + yCH_3^+ \quad (3)$$

(with integers $x \geq y > 0$).

With molecular iodine however, charge balancing from the environment is required. This can for instance involve a hydrogen ion from the decomposition of a water molecule:

$$xM^{a+}_{(s)} + (a/2)I_{2(g)} + H_2O_{(g)} \rightarrow xMI_{a(s)} + H^+_{(s)} + OH^- \quad (4)$$

Sorbents can also have salts as active sites, most commonly nitrates. Reactions with molecular and organic iodine generate nitrogen oxides (NOx) as follows:

$$xM(NO_3)_{y(s)} + (a/2)I_{2(g)} \rightarrow xMI_{a(s)} + NOx_{(g)} \quad (5)$$

$$xM(NO_3)_{y(s)} + yCH_3I_{(g)} \rightarrow xMI_{y(s)} + NOx_{(g)} + \text{hydrocarbons}_{(g)} \quad (6)$$

4. Silver mordenites

Mordenites (MORs) are porous aluminosilicate zeolites with the chemical formula $(Ca,Na,K_2)Al_2Si_{10}O_{24}\cdot 7H_2O$ and an orthorhombic structure (Cmcm space group) [42]. After cationic exchange with silver ions, Ag^+-MORs can be used as iodine sorbents, while after H_2 treatment, the metallic silver in Ag^0-MORs behaves as an active site.

4.1. Location and insertion of silver into mordenites

Structurally, mordenite (Figure 1) consists of several cages occupied by cations (Na^+, Ca^{2+}, K^+). Mordenites are the most studied zeolites for iodine adsorption because they are stable in acid gases (radioactive iodine is generated in a nitric acid environment) and because they are one of the rare zeolites that can be synthesized with a wide range of Si/Al ratios [43,44]. This ratio is important because it allows the cation content of the structure to be adjusted without modifying the crystal structure or lattice parameters [45]. The cation content of the structure, and thus its Ag^+ content, is inversely proportional to the Si/Al ratio. As shown in Figure 1, silver ions can occupy several different sites in the structure.

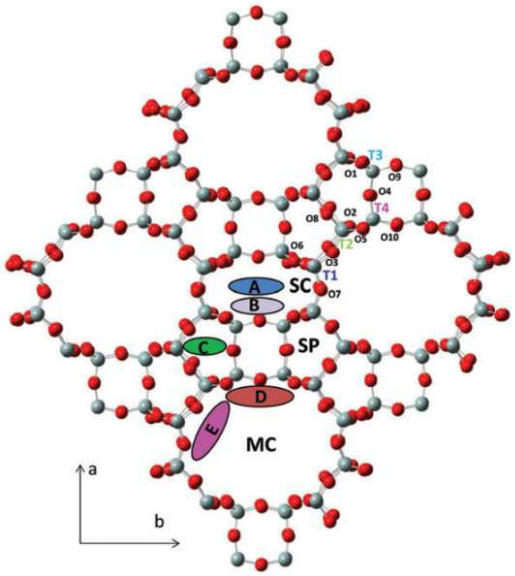

Figure 1. Crystal structure of mordenite with the main channel (MC), side channel (SD) and side pocket (SP). Ag^+ cations can occupy the sites indicated by capital letters (A-E) and Al atoms occupy the tetrahedral sites T1–T4. (Si atoms in grey, O in red) [45].

Ag^+-MOR is usually transformed into Ag^0-MOR by heating in flowing H_2.This leads to the substitution of Ag^+ by H^+ and the migration of the former to the surface of the material where it forms silver metal nanoparticles [46–48].

4.2. Iodine capture performance of Ag^+-MORs

The iodine capture properties of Ag^+-MORs in the presence of contaminants have been studied by DFT modelling. Chibani et al. calculated the mean interaction energies between Ag^+-MORs and different compounds (I_2, CH_3I, CO et H_2O) as a function of the Si/Al ratio (and thus the Ag^+ content; Figure 2a) [45]. Their results show that at low Ag^+ contents (Si/Al ratios of 47 and 23), the interaction energies of iodine species are slightly lower than those of water molecules and of CO, suggesting a competition effect, in particular with CO, as described for faujasite by Chebbi et al. [49]. Reducing the Si/Al ratio (down to 11 or 5), leads to a substantial decrease in the interaction energies with iodine species, while those for CO and H_2O remain almost unchanged. This implies that increasing the Ag^+ content of mordenites favours interactions with iodine species over those with CO and H_2O.

The results of a similar study [50] involving different organic contaminants such as methane (CH4), cyclohexane (C_6H_{12}) and methanol (CH_3OH), shown in Figure 2b,c, indicate that iodine can only be selectively captured in the presence of these organic compounds at the very lowest Si/Al ratios (here, 5). These studies show that contaminants (H_2O, CO, hydrocarbons etc.) typically have a negative effect on the performances of Ag^+-MORs.

The capture properties of Ag^+-MORs for CH_3I were studied under dynamic conditions using breakthrough experiments at 100°C [51]. Sorbents containing 5.9 and 7.3 wt.% silver were found to capture 82 and 120 $mg \cdot g^{-1}$ of iodine respectively (28 and 34% of which was physisorbed), indicating that the amount of iodine captured is proportional to the silver content of the sorbent, although a considerable proportion is physisorbed.

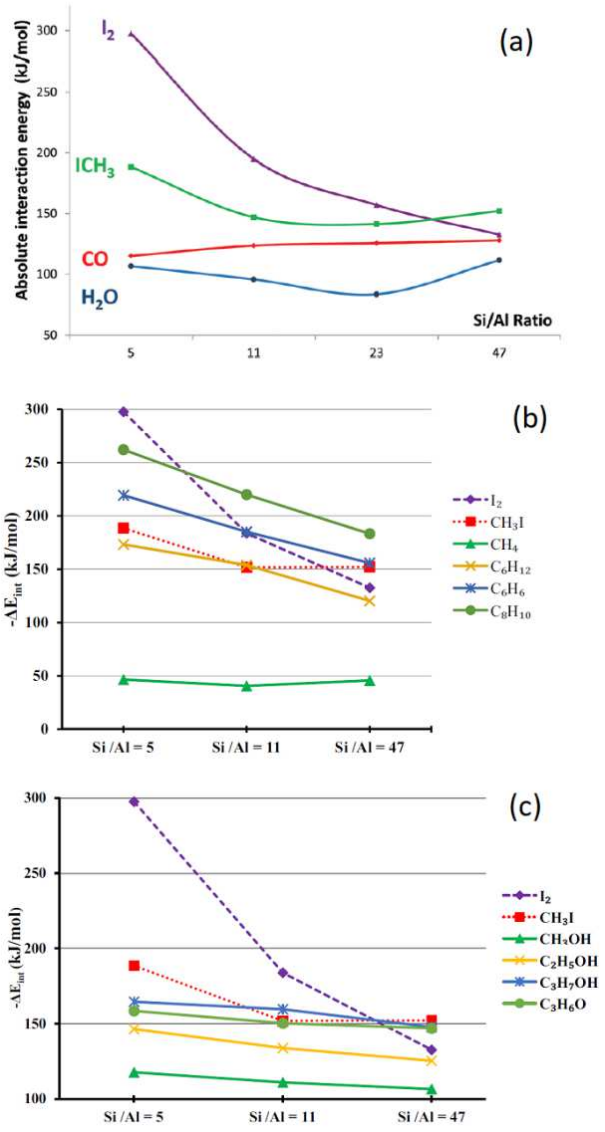

Figure 2. (a) Average interaction energy in absolute value between Ag^+-mordenites with several Si/Al ratios and different gaseous compounds [45]. (b,c) Evolution of the interaction energies of Ag^+-mordenites with (b) iodine compounds and hydrocarbons or (c) oxygenated compounds, as a function of the Si/Al ratio [50].

4.3. Iodine capture performance of Ag^0-MORs

Scheele et al. used a specific fixed bed capture setup with a mixture of CH_3I and air percolating through a column filled with sorbent to study the iodine capture efficiency of Ag^0-MORs [48]. Several parameters were varied, such as the temperature (from 86 to 200°C), the gas flow rate (3.75 to 15 $m \cdot min^{-1}$) and the presence or not of NO and NO_2.The maximum

capacity of the sorbents was found to be proportional to temperature and inversely proportional to the gas flow rate and the amount of NOx present. A reasonable explanation for these results is that NOx reacts with active sites thereby reducing the sorbent's capacity for iodine. Meanwhile, increasing the flow rate reduces the contact time of iodine with the active sites, and thus presumably also the capture rate. The variation with temperature is harder to explain. Under optimal conditions (200°C, 3.75 $m \cdot min^{-1}$ flow rate, no NOx), the iodine sorption capacity was 217 $mg \cdot g^{-1}$. In the presence of contaminants (NOx and H2O) and at 150°C, the sorption capacity was found to be 52 $mg \cdot g^{-1}$[52].

In another study focussing on I_2 capture under dynamic conditions (without NOx) [47], Ag^0-MORs were found to capture 115, 135, and 100 $mg \cdot g^{-1}$ on average at 100, 150 and 200°C, respectively. The authors state that the loading capacity should decrease as the temperature increases, but between 100 and 150°C the opposite was observed. The proposed explanation is that the water initially present in Ag^0-MOR hinders I_2 capture by reacting with Ag^0. Since there is more water in the structure at lower temperatures, this explains why more iodine is captured at 150°C than at 100°C. Another interesting result of this study is that the proportion of chemisorbed iodine decreases from 97 to 91% between 100 and 200°C.

4.4. Differences between Ag^+- and Ag^0-MORs

The oxidation state of Ag in these sorbents has a direct effect on the iodine adsorption capacity and the types of AgI crystals formed. Nan et al. demonstrated this behavior by modulating the H_2 reduction treatment (170 up to 500 °C during 24 up to 336 h) of the sorbents and therefore the Ag^0 content to the detriment of Ag^+ [47]. After 24 h reduction at 230°C, the iodine adsorption capacity measured in a continuous flow setup (temperature not specified) was 65 $mg \cdot g^{-1}$, whereas after 24 h at 400°C (complete reduction) the adsorption capacity was 105 $mg \cdot g^{-1}$. There is therefore an increase of iodine loading capacity when the

quantity of Ag^0 increases explained by a better accessibility of iodine with active sites principally localized on the surface [46–48].

Regarding the crystal structure of the silver iodide produced, Chapman et al. [53] found that below 147°C, a single β-AgI phase (with wurtzite structure) forms regardless of the oxidation state of the silver (Ag^0 or Ag^+). However, this is not the case at higher temperatures. In the presence of Ag^0, two phases form: α-AgI (body-centered cubic structure) and a metastable γ phase. The crystallites of the α-phase are sub-nanometer in size and found on the inside of the pores in the Ag^0-MOR while the crystallites of γ-AgI are micrometer scale and found on the surface. In the presence of Ag^+, only the α-phase forms and is found exclusively in the pores. Thus, while Ag^+-MORs capture less iodine than Ag^0-MORs, the AgI crystallites that form in the former are all nanoconfined inside the structure.

4.5. Conversion of iodine-loaded Ag^0-MORs into stable waste forms

The conversion of iodine-loaded Ag^0-MOR into waste forms by hot pressing has been studied at Oak Ridge National Laboratory [54]. Preliminary tests using hot uniaxial pressing (HUP, at 750°C at 27.5 MPa) on sorbents without iodine showed that the pressure with this technique was insufficient to collapse the mordenite pores and that the resulting materials were too friable (Figure 3a). However, thanks to the higher pressures achievable by hot isostatic pressing (HIP) (175 MPa at 525°C), the materials obtained (in galvanized steel containers) were monolithic, compact and non-friable, and consisted of a mixture of crystalline (AgI and $Ag(IO_4)$) and amorphous regions. Furthermore, no iodine volatilization was detected. HIP at 700°C produced the same results (Figure 3b). However, the chemical durability of this waste form was not studied. It is also possible to convert these sorbents (and more generally temperature sensitive sorbents) by densification at ambient temperature [55]. By mixing them with ductile metallic powder (Sn, Au, Cu …), a compacted metallic matrix

215 which encapsulates the iodine-loaded sorbents can be obtained after uniaxial pressing at
216 172 MPa.
217 Another method that has been studied to transform these sorbents into stable waste forms is to
218 mix them with a low sintering temperature glass. Garino et al. mixed AgI-MOR with Bi_2O_3-
219 SiO_2-ZnO glass powder at 20/80 wt.% [56]. Metallic silver was added in excess (5 wt.%) to
220 capture any iodine (most likely the physisorbed portion) released during the treatment. The
221 mixture was uniaxially pressed at 70 MPa to form pellets that were then heated at 550°C for
222 1 h. Cohesive multiphase materials were obtained, consisting of amorphous, $Bi_4(SiO_4)_3$,
223 mordenite and AgI phases, in the form of a composite AgI-MOR core, glass shell matrix, as
224 shown in Figure 3c. The thermal treatment led to partial crystallization of the glass into
225 $Bi_4(SiO_4)_3$, and transformation of metallic silver into AgI. Chemical durability tests performed
226 for 7 days in deionized water (15 mL for 1.5 g of sample) at 90°C indicates that the element
227 detected at the highest concentration in solution was boron, at 8.6 ppm.

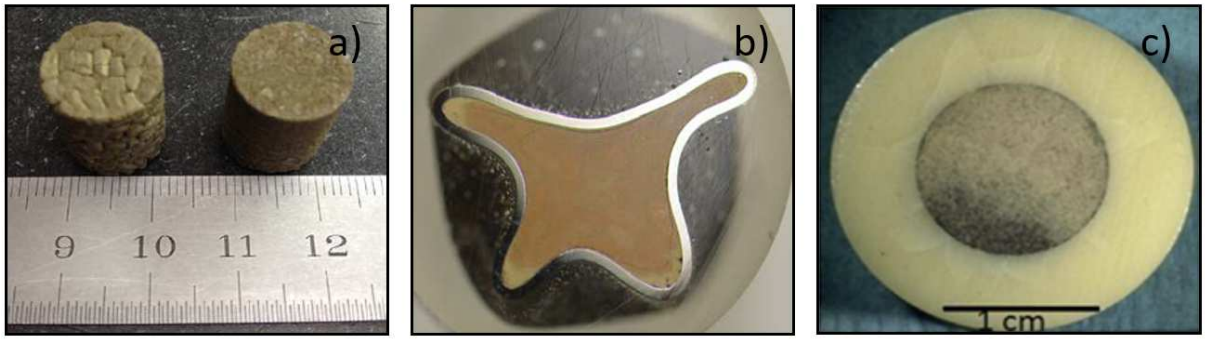

228

229 **Figure 3 .** (a) Photograph of AgI-mordenite matrices obtained from (left) pellets and (right) powder
230 after hot uniaxial pressing at 750°C and 27.5 MPa [54,57]. (b) Photograph of a AgI-mordenite matrix
231 obtained after hot isostatic pressing at 700°C and 175 MPa [54,57]. (c) Photograph of a sintered
232 core/shell matrix with a 100% glass shell and glass/AgI-mordenite/Ag core [56].
233
234 The different techniques presented above and more specifically the densification at ambient
235 temperature [55] can potentially be used on faujasites, another kind of porous aluminosilicate

belonging to zeolite family. Several works have demonstrated the performances of silver-faujasites both for I_2 and CH_3I trapping [51,58–61].

5. Silver-silica aerogels

Aerogels are extremely porous semi-rigid materials with very high specific surface area (sometimes greater than 1000 $m^2\ g^{-1}$) and containing more than 90 wt.% air [62,63]. They are composed mainly of carbon materials, silicon and metal oxides and are good candidate materials for the capture and immobilization of gaseous iodine.

5.1. Iodine capture performance and aging of silver-silica aerogels with thiol functions

In this context, silver-silica aerogels have been functionalized with thiol functions by reaction with silane-thiol (Si-SH) groups [64]. When the sorbent is impregnated with an $AgNO_3$-containing solution, these thiol functions lead to the formation of silver complexes (S-Ag bonds) in the structure, such that the silver is covalently bonded to the silicon network. Ag^0-based sorbents are finally obtained after thermal treatment under argon/H_2. In dynamic I_2 adsorption experiments in humid air at 150°C, these sorbents captured 480 $mg{\cdot}g^{-1}$ iodine in 11 days, with very little physisorption (less than 10 $mg{\cdot}g^{-1}$) [64]. In iodine release experiments performed after 2 months' storage in the laboratory (at ambient temperature and pressure), the sorbents released 15% of the captured iodine under static conditions (at 150°C in air containing 2 vol.% NO_2) [65] and 43% under dynamic conditions (flowing air + 1 vol.% NO) [66]. Over 6 months' storage in humid air, without NOx, around 22 wt.% of the iodine was released [66].

Thus, although these sorbents capture iodine by chemisorption, the iodine seems to be released as they age under the effect of different gaseous species. The stability of the sorbents over time is therefore an important consideration to limit iodine release.

Matyas et al. studied the ageing process in these aerogels (in the absence of iodine) in different gases (air, H_2O and NO) at 150°C [67]. In the presence of NO, the surface thiol groups are oxidized, leading to the formation of R-SO_4 sulphate groups. In air (dry or humid), some of the thiol groups become oxidized to sulphate and silver sulphate is produced. This is the proposed mechanism through which AgI becomes destabilized and the material is thought to age.

5.2. Iodine capture performance of silver-silica aerogels without thiol functions

Riley et al. prepared Al-Si-O and Na-Al-Si-O aluminosilicate aerogels impregnated with $AgNO_3$ for I_2 capture [68]. While the Ag loading efficiency of the Al-Si-O aerogels was low, with few silver active sites on the surface, limiting the iodine adsorption capacity, the impregnation of the Na-Al-Si-O gels was much more efficient, with Ag^+ replacing Na^+ ions in the structure by cationic exchange (as in mordenites). In iodine loading tests performed in an iodine-saturated chamber at 150°C, the iodine sorption capacity of the Na-Al-Si-O aerogels was measured at 517 $mg \cdot g^{-1}$ and at 555 $mg \cdot g^{-1}$ after reduction of the Ag^+ to Ag^0 by heat treatment under argon/H_2. The ageing behaviour of these sorbents was not studied however.

5.3. Conversion of iodine-loaded silver-silica aerogels into stable waste forms

Matyas et al. have studied the effects of densification on silver-silica aerogels with thiol functions as a means to immobilize captured molecular iodine [69]. After HUP (1200°C, 29 MPa), the measured residual open porosity was 17% with 7% iodine loss. After HIP (1200°C, 207 MPa), with the sorbent encased in a metal canister, 100% densification was obtained and

no iodine release was detected. HIP therefore seems to be the best option to densify iodine-loaded aerogels. Scanning electron microscopy (SEM) analysis of these material's microstructure after sintering revealed four separate phases, identified by X-ray diffraction (XRD) as an amorphous silica-based phase, metallic silver, Ag_2S, and AgI. The chemical durability of this waste form was not studied.

6. Silver silica and silver alumina

Solid supports based on mesoporous alumina (Al_2O_3) or silica (SiO_2) impregnated with silver nitrate are some of the earliest-studied materials for gaseous iodine capture [28,70]. These sorbents are now widely used in nuclear reprocessing plants.

6.1. Iodine capture performance of silver silica

Solid sorbents based on silica impregnated with silver nitrate were developed in Germany in the 1970s for the Kalshruhe pilot reprocessing plant (WAK, shut down in 1992) to comply with regulations on iodine release into the atmosphere [71]. These sorbents, sold under the name AC-6120, are prepared as small beads, 1–2 mm in diameter and have a specific surface area of 65–110 $m^2\ g^{-1}$, a pore size distribution of 20–40 nm and a maximum Ag^+ content of 12 wt.% [28]. Decontamination factors (DFs, the ratio of the concentration or activity of the gaseous iodine before and after passing through the sorbent) greater than 99% have been measured in laboratory-scale fixed bed adsorption experiments for I_2 in air containing 1–5 vol.% NO_2 [72]. The removal efficiency is substantially lower at high levels of humidity however, dropping from 99% at 70% relative humidity to 27% at 100% relative humidity. These sorbents were successfully used in the WAK plant to remove at least 90% of the iodine from the off-gas [71].

6.2. *Conversion of iodine-loaded silver silica into stable waste forms*

Wada et al. used HIP (750°C, 100 MPa) to densify 13.2 wt.% iodine-loaded silver silica, achieving a volume reduction of 48% [73]. No iodine release was detected during the treatment. The waste form obtained (Figure 4) consisted of SiO_2, Ag, and AgI phases, indicating that the iodine was retained as silver iodate and did not enter the silica matrix. The chemical durability of this waste form was not investigated however.

Figure 4. Photograph of an iodine-loaded silver-silica waste form obtained by hot isostatic pressing at 750°C and 100 MPa [73].

6.3. *Iodine capture performance of silver alumina*

Silver-loaded alumina sorbents were developed in Japan in the 1980s for the Tokai reprocessing plant (shut down in 2014) [28]. These sorbents in the form of beads roughly 2 mm in diameter can carry up to 24 wt.% silver and their physical properties are similar to those of the silver-silica beads described in the preceding paragraph. In laboratory-scale experiments at 150°C under dynamic conditions with flowing air containing CH_3I, the iodine sorption capacities of materials with 10 and 24 wt.% Ag were measured at 100 and 230 mg g^{-1} [74]. Experiments performed under the same conditions but this time with I_2 yielded similar results, with a sorption capacity of 220 mg g^{-1} for the material loaded with 24 wt.% Ag [75]. The extraction performance seems therefore to depend little on the form of the iodine. It was also shown that 78% of the silver in the material reacted with iodine to form

AgI and the DF was found to be proportional to temperature over the range 25–150°C. The authors suggest that this is because iodine and silver are less likely to interact at lower temperatures [75]. In another study however, the performance of these sorbents for I_2 under dynamic conditions was found to vary little with temperature over 100–650°C except for a drop at the highest temperature [76]. This is likely because the silver had melted (above 558°C), leading to volatilization of the iodine. This is in keeping with iodine release tests performed on AgI-loaded sorbents, which showed weight loss starting from about 530°C [75]. Studies have also shown that when the pores inside the material are too small, the DF of these sorbents tends to decrease as the relative humidity of the environment increases, [77,78]. Indeed, capillary condensation leads to pores smaller than 50 nm becoming filled with water molecules, preventing any contact between the gaseous iodine and the silver active sites and reducing the sorption efficiency. This effect does not occur in pores larger than 50 nm, explaining why the efficiency of sorbents with pores mainly 40–70 nm in diameter was maintained at more than 95% at a relative humidity of 95% [77].

6.4. Conversion of iodine-loaded silver-alumina into stable waste forms

These sorbents can be stabilized by HIP treatment. Figure 5 from Masuda et al. [79] shows that after thermal pretreatment at 480°C (to remove contaminants), and HIP at 175 MPa and 1200°C, the concentration of silver (aluminium) is much higher (lower) in the core of the sample than on the outside. This is consistent with the presence of two phases, namely AgI mainly in the center and Al_2O_3 mainly on the outside.

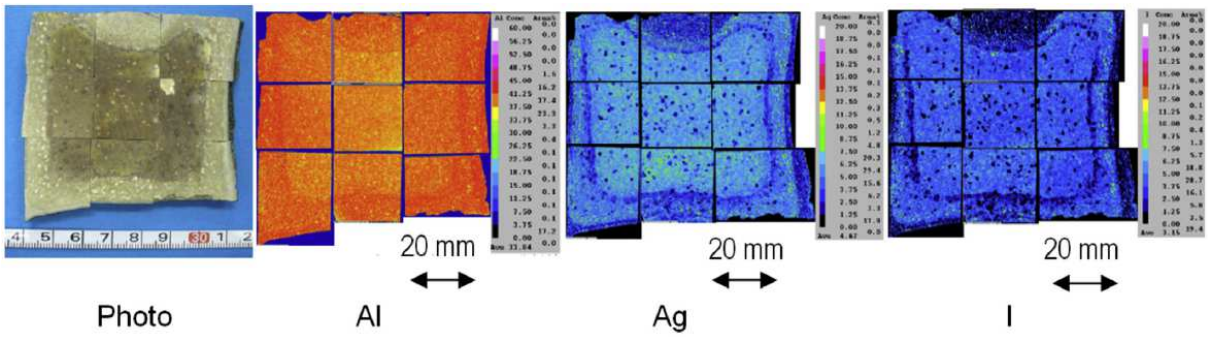

Figure 5. Cross-sectional photograph of an iodine-loaded silver-alumina sorbent after hot isostatic pressing (1200°C, 175 MPa) and the corresponding elemental distributions measured by electron probe microanalysis [79].

By adding a second pretreatment step, in a vacuum ($< 7 \times 10^{-2}$ Pa) at between 400 and 500°C, Matsuda et al. were able to reduce the void volume inside the densified waste from 15 vol.% to less than 5 vol.% [79].

7. Lead-bismuth

7.1. Mechanism of iodine capture

Lead bismuth-based sorbents have been developed by Mukunoki et al. [80] to regenerate primary sorbents. This process involves treating loaded gaseous iodine sorbents (for example, Ag-based sorbents) **under** H_2 flow to reduce and desorb the iodine. The released gaseous iodine is then captured in a $BiPb_2O_2NO_3$ sorbent by ion exchange via the following reaction:

$$BiPbO_2NO_3 + I^- \rightarrow BiPbO_2I + NO_3^- \quad (7)$$

7.2. Conversion of iodine-loaded lead-bismuth

Once loaded with iodine, the second sorbent is mixed with ZnO and vitrified at 540°C (low enough to ensure no iodine is released) producing a homogenous glass with 2 wt.% iodine [80]. In chemical durability tests performed at ambient temperature in a reducing

environment, the formation of an alteration layer on the surface of the glasses was observed, which should favour iodine retention, particularly in basic environments. These results are difficult to interpret however.

8. Chalcogels

8.1. Iodine capture performance

Chalcogenide-based aerogels (chalcogels) with chemical formula Sn_2S_3 (SnS) and $Sb_{13.5}Sn_5S_{20}$ (SbSnS) are another type of material that has been developed to trap and immobilized iodine [81]. In static I_2 capture tests performed under vacuum in desiccators (temperature not specified), the loading capacity of the SnS sorbent reached 680 $mg \cdot g^{-1}$. In powder form, the sorbents became saturated after about 5 days and in the form of granules, after about 20 days. This is because the pores are much more accessible in the powder. With the SbSnS sorbent, the sorption capacity was measured at 540 $mg \cdot g^{-1}$, and the conclusions regarding the physical form of the sorbent (powder or granular) were the same. X-ray diffraction data showed the presence of several iodine-containing phases, SnI_4 and $SnI_4(S_8)_2$ in the SnS sorbent, and SbI_3 and $SbI_3(S_8)_3$ in the SbSnS sorbent.

Subrahmanyam et al. have also investigated chalcogels for iodine capture [82]. They notably developed a $Zn_2Sn_2S_6$ sorbent with a specific surface area of 400 $m^2 \cdot g^{-1,}$ a wide range of pore sizes (from micro to macroscale) and tin active sites that react with iodine by chemisorption to form SnI_4. The sorption capacity of this material for I_2 was measured at 2250 $mg \cdot g^{-1}$ in a sealed nitrogen environment at 60°C, and 1970 $mg \cdot g^{-1}$ in static conditions under vacuum at 22°C. The authors explain the lower performance in the second test by surface oxidation due to prolonged exposure to air during preparations, which reduced the number of tin active sites. Subsequent thermogravimetric analysis of sorbents with and without iodine (Figure 6) showed weight loss of about 70% between 150 and 200°C, indicating iodine release from the melting

386 of SnI_4 at 143°C. A further 10% of the initial weight was lost between 200 and 400°C,
387 corresponding to the volatilization of SnI_4 at 348°C.

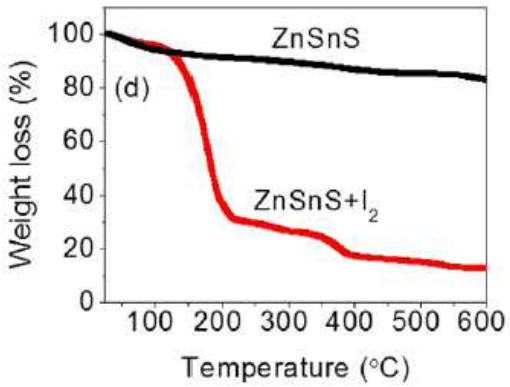

388

389 **Figure 6.** Thermogravimetric analysis of $Zn_2Sn_2S_6$ before and after iodine capture [82].

390 ## *8.2. Conversion of iodine-loaded chalcogen into stable waste forms*

391 Since SnS does not form a glass by itself [83,84], Riley et al. investigated the possibility of
392 vitrifying their SnS sorbents after adding germanium [81]. The precursors were sealed inside a
393 quartz tube and heated for 10 min at 400, 500 and 600°C, leading to the release of black
394 fumes inside the tube. Figure 7a shows the samples before and after heat treatment. X-ray
395 diffraction analysis revealed the presence of an amorphous phase, SnI_4 (corresponding to the
396 yellow areas in Figure 7a), SiO_2 (from the quartz tube) and GeS_4. Energy dispersive X-ray
397 spectroscopy (EDS) showed that 24 at% of the iodine was in the amorphous phase. The
398 chemical durability of this potential waste form was not studied.
399 The SbSnS sorbent was consolidated directly in a sealed quartz tube with the sampled placed
400 inside a glassy carbon crucible to avoid any SiO_2 entering the final waste form [81]. No
401 germanium was required in this case because the Sb-Sn-S-I system forms a homogeneous
402 glass at 600°C. Red fumes were observed in the tube when the sample was taken out of the
403 oven after 3 h at 600°C. The material obtained after a second heat treatment at 500°C is
404 shown in Figure 7b. X-ray diffraction and EDS showed the presence of several crystalline
405 phases such as SbSI, SbI_3 and SiO_2 as well as heterogeneities linked with the porous nature of

406 the material. The vitrification conditions tested here do not therefore produce a dense and
407 homogeneous immobilization matrix.
408 Similar tests were performed on iodine loaded $Zn_2Sn_2S_6$ sorbents with the aim of transforming
409 them into solidified waste [82]. Sb_2S_3 was added to promote the formation of a homogeneous
410 glass. The precursors were heated at 600°C and then water quenched. The contents of the
411 quartz tube before and after heat treatment are shown in Figure 7c. The presence of orange
412 deposits on the side of the tube after heat treatment is a sign of volatilisation. The final glassy
413 material was found to consist mainly of antimony and sulfur, with 25 wt.% iodine and small
414 amounts of zinc and tin, indicating a type of ternary Sb-S-I glass [85]. The residues on the
415 side of the tube were found to contain SbI_3 and SbSI. The chemical durability of this potential
416 waste form has not been studied.

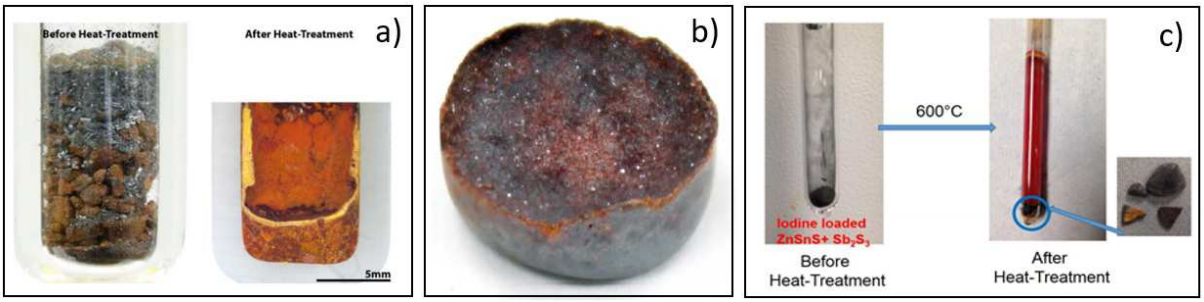

417

418 **Figure 7.** (a) Photographs of iodine-loaded SnS filters mixed with GeS_2 (left) before heat treatment
419 and (right) a polished cross-section after heat treatment [81]. (b) Photograph of iodine-loaded SbSnS
420 filters after vitrification at 600 °C [81]. (c) Photograph of iodine-loaded $Zn_2Sn_2S_6$ filters after
421 vitrification at 600 °C [82].

422 ## 9. Metal organic frameworks (MOFs)

423 Metal–organic frameworks (MOFs) are hybrid organic-inorganic crystalline materials
424 consisting of metal ions or clusters coordinated by organic ligands and forming organized 1D,
425 2D, or 3D structures with specific surface areas that can be as high as 10^4 $m^2 \cdot g^{-1}$. Their high

porosity and the large quantities of different structures make them often considered for iodine trapping [35].

9.1. Iodine capture performance of ZIF-8 and HKUST-1

The MOFs that have been studied the most for iodine gas capture are the ZIF-8 and HKUST-1 (also known as Cu-BTC) classes, whose crystal structures are shown in Figure 8. Zeolite imidazolate frameworks (ZIFs) consist of zinc tetrahedra connected by imidazolate linkers and HKUST-1 (Hong Kong University of Science and Technology) is made up of copper dimers connected by trimesic acid linkers.

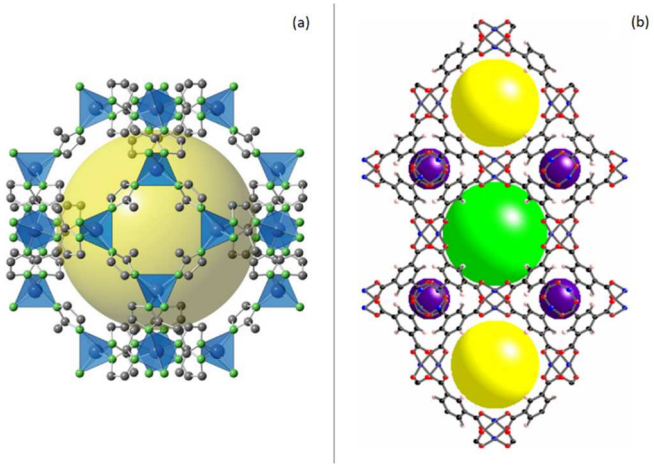

Figure 8. Crystal structures of (a) ZIF-8 (Zn^{2+} in blue, N in green, C in grey ; the yellow sphere is a pore) and (b) HKUST-1 (Cu^{2+} in blue, O in red, C in black and H in pink ; the yellow, green and purple spheres are pores of different sizes) metal-organic frameworks [86,87].

Sava et al. have shown that ZIF-8 can capture up to 1250 $mg \cdot g^{-1}$ I_2 when placed inside a hermetically adsorption chamber at 77°C and ambient pressure [88]. Under the same experimental conditions, Chapman et al. measured an iodine loading of 1200 $mg \cdot g^{-1}$ [89]. These results are in keeping with the maximum loading level of 1487 $mg \cdot g^{-1}$ calculated using Monte-Carlo simulations [90]. The temperature in these simulations was 25°C and dynamic effects were ignored. In a more recent combined experimental and modelling study [91], the

two approaches yielded similar results for I_2 capture at 75°C and 1.17 bar, with loading capacities of 1100 $mg \cdot g^{-1}$ (calculated) and 1170 $mg \cdot g^{-1}$ (measured under static conditions). MOFs are usually used in a powdery form. This is why Tang et al. worked on a way to transform them into easily usable sorbents [92]. They made a mixed membrane sorbents by mixing ZIF-8 with polyethersulfone. In their initial form, ZIF-8 can trap iodine with a capacity of 876 $mg \cdot g^{-1}$ (temperature not specified) whereas after transformation, they can reach 1387 $mg \cdot g^{-1}$. This modification has the double beneficial effect of increasing the capacity (supposed to be related with the increase of void volume) and making these sorbents easily usable which is important at industrial scale.

For HKUST-1, the combined experimental and modelling study was also carried out [91]. The loading level predicted by simulations was much higher than the experimental measurements under static conditions (1450 vs 760 $mg \cdot g^{-1}$) [91]. The authors suggest that this discrepancy may be due to differences in pore sizes. Indeed, while in HKUST-1 the large cavities and pore apertures are respectively 14 and 10 Å in diameter, the pores in ZIF-8 are much smaller (respectively 11.6 and 3.4 Å across) [88,93]. This means that physisorbed iodine is more likely to desorb in HKUST-1 than in ZIF-8. Furthermore, I_2–framework interactions were estimated to be weaker in HKUST-1 than in ZIF-8. Under the same experimental conditions but with a relative humidity of 3.5%, Sava Gallis et al. measured an iodine sorption capacity of 1750 $mg \cdot g^{-1}$ [36], indicating that at low concentrations, water vapor promotes iodine capture but does not alter the selectivity of HKUST-1.

The iodine sorption performance of HKUST-1 and ZIF-8 have also been studied under dynamic conditions. Chebbi et al. measured sorption capacities of 1425 and 7 $mg \cdot g^{-1}$ for HKUST-1 and ZIF-8, respectively, in CH_3I sorption tests performed at 35°C until saturation (for up to 130 min) [94]. For HKUST-1, the results are similar to those measured in static experiments [36]. For ZIF-8 however, the authors explain the very low iodine loading

capacity by the large CH_3I molecules (5–6 Å) being unable to pass through the narrow pore apertures (3.4 Å) in the structure. This drastic drop in efficiency is therefore due to the use of CH_3I (instead of I_2 for the static experiments) rather than the dynamic nature of the experiments. These results show that while ZIF-8 is only well suited to trap I_2, HKUST-1 can be used to trap iodine in both molecular and organic form.

9.2. Temperature dependence of iodine retention

Transforming sorbents into stable waste forms often requires heating to eliminate pores in the structure. Understanding the temperature behaviour of iodine-loaded sorbents is therefore important because there are no active functions involved. Using thermogravimetric analysis, Sava et al. [88] observed that weight loss in their iodine-loaded sorbents began at 120°C regardless of the iodine content. Indeed, I_2 trapped by physisorption is much more thermally unstable than chemisorbed iodine. Thereafter, the thermal decomposition of ZIF-8, which begins at around 302°C inevitably leads to the release of the remaining iodine, even the portion trapped in the smallest pores [95,96]. Bennett et al. [97] have nevertheless shown that the thermal stability of these materials can be increased, and iodine release reduced, by ball milling for 30 min at 25 Hz, which collapses the porous network. Thermogravimetric analysis of the sorbents before and after ball milling (Figure 9) showed that mass loss in the (amorphous) treated sorbents only began above 200°C and that iodine was only completely released at about 425°C, compared with about 350°C in the (crystalline) untreated material. These results highlight how pore closure acts as a physical barrier against iodine release.

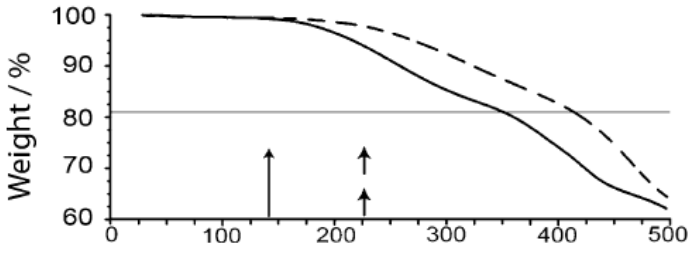

Figure 9. Thermogravimetric analysis of iodine-loaded ZIF-8 before (solid line) and after (dashed lined) ball milling [97].

Similar results have been described for HKUST-1, with iodine release beginning at temperatures as low as 150°C [36] and completed at about 250°C with the thermal decomposition of the network.

Despite this physisorption phenomenon, MOFs look promising as reversible sensors to detect gaseous iodine, even at very low concentration, for nuclear site monitoring [98–100].

9.3. Conversion of MOF-glass composites into stable waste forms

Sava et al. investigated coating with Bi_2O_3-ZnO-B_2O_3 and Bi_2O_3-ZnO-SiO_2 glass powders as a means to transform these MOFs into durable glass-composite waste forms [101]. The MOFs (10 wt.%) were mixed in a mortar and pestle with glass powder (80 wt.%) and metallic silver (10 wt.%), included to capture (as AgI) any iodine released during the treatment process. The pellets were then heat treated at 500°C, forming dense, cohesive monoliths (Table 1, Figure 10).

Table 1. Characteristics of iodine-loaded sintered glass composite materials [101]

Sample	Precursors	Phases
Glass composite 1	Bi_2O_3-ZnO-B_2O_3 + ZIF-8	BiOI + BiI_3 + Ag^0 + AgI
Glass composite 2	Bi_2O_3-ZnO-B_2O_3 + HKUST-1	BiOI + $Bi_{12}SiO_{20}$ + Ag^0 + AgI
Glass composite 3	Bi_2O_3-ZnO-SiO_2 + ZIF-8	Amorphous area + Ag^0 + AgI
Glass composite 4	Bi_2O_3-ZnO-SiO_2 + HKUST-1	Amorphous area + Ag^0+ AgI

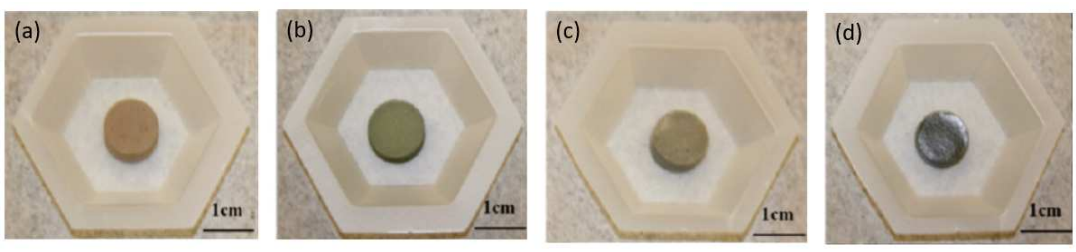

Figure 10. Photographs of iodine-loaded sintered glass composite materials [101], produced from (a) Bi_2O_3-ZnO-B_2O_3 + ZIF-8, (b) Bi_2O_3-ZnO-B_2O_3 + HKUST-1, (c) Bi_2O_3-ZnO-SiO_2 + ZIF-8 and (d) Bi_2O_3-ZnO-SiO_2 + HKUST-1 precursors.

No iodine release was detected during heat treatment, which usually is the main limitation of this process. Table 1 shows that all four glass composites contained Ag^0 and AgI. However, whereas the composites prepared using Bi_2O_3-ZnO-SiO_2 powder had amorphous areas, those prepared with Bi_2O_3-ZnO-B_2O_3 contained several crystalline phases. The presence of iodine in the amorphous regions was not studied. Thermogravimetric analysis showed that they remained stable up to 500°C, with less than 1% weight loss. After chemical durability tests performed in 10 mL deionised water at 90°C for 7 days, inductively coupled plasma–mass spectrometry analysis of the supernatant revealed detectable concentrations of iodine only for glass composite 1 (97 ppm, Table 1). This is because crystalline BiI_3 is partially soluble in water [102]. Longer tests performed under reducing conditions would be interesting to establish whether these glass composites can be used for deep geological disposal.

9.4. Conversion of other MOFs designed for iodine trapping

The previous paragraph demonstrates the possibility of transforming iodine-loaded MOFs (HKUST-1 and ZIF-8) into glass composite conditioning matrices. In that case, metallic silver is used to chemisorb iodine that had been initially trapped in the MOFs (by formation of AgI) and glass powder precursors act as a physical and chemical barrier to prevent iodine release (encapsulation). Thereby, even if the different phases formed in the final matrices can be linked to the intrinsic nature of the MOF (metals, organic linkers …), this process seems to be transposable to other types of existing MOFs. A recent review on the different MOFs designed for gaseous iodine trapping (and in solution) has been published by Xie et al. [35].

Hereafter, other works (published after the review of Xie et al.) dealing with the trapping of gaseous iodine are also discussed.

Chen et al. focused their work on Zr-based MOFs because of their versatility to be synthetized with various organic linkers [103]. Their iodine capture tests in static conditions at 80 °C reveal a capacity of 2180 $mg \cdot g^{-1}$ for MOF-808 and 1450 $mg \cdot g^{-1}$ for NU-1000. These high capacities are directly linked to high specific surface areas (1930 and 2126 $m^2.g^{-1}$ respectively) and are due to high connectivity between pores and rigid organic linkers. On the other hand, UiO-67 and MOF-867, which have higher specific surface areas (2638 and 2403 $m^2.g^{-1}$ respectively), are less efficient for iodine trapping in the same conditions (530 and 880 $mg \cdot g^{-1}$ respectively). Their lower connectivity and the nature of the flexible organic linkers can explain these results. Other tests with relative humidity of 18 % showed a sharp decrease of around 70 % of the maximum loading for all previous MOFs. Among Zr-based MOFs, UiO-66 also demonstrated a capacity of 660 $mg \cdot g^{-1}$ in static conditions at 80 °C [103]. To improve the efficiency of UiO-66, some works focused on their chemical modification by adding organic linkers to increase electro-donating properties [104,105]. These modifications made it possible to reach a capacity of 1330 $mg \cdot g^{-1}$ in static conditions at 75 °C. However, the highest capacity obtained for UiO-66 sorbents was finally obtained thanks to the presence of defects in the structure [106]. In that case, iodine capture tests in static conditions at 80 °C reveal a capacity of 2250 $mg \cdot g^{-1}$. Leloire et al. also demonstrated the interest of using UiO-66-NH_2 sorbents (UiO-66 functionalized with NH_2 groupements) in severe nuclear conditions [107]. Their millimetric spherical sorbents (size range of 0.5-1.4 mm) made with a binderless method were irradiated under doses of 2 MGy of gamma irradiation. The results indicated the conservation of their size and structure. Moreover, others irradiation tests were carried out on the same sorbents but loaded with radioactive iodine. After 30 h of exposure under a flow of irradiated air (1.9 $kGy.h^{-1}$) at 120 °C, 3.5 bar and 20 % of relative humidity, no radioiodine

558 was released which proves the stability of these materials under simulated nuclear accidental
559 conditions.
560 A new kind of MIL-101 was studied in the presence (or not) of Cu nanoparticles encapsulated
561 inside them to improve their chemical affinity with I_2 [108]. The different tests done in static
562 conditions at 77 °C (up to 12 h) showed a capacity of 3000 $mg \cdot g^{-1}$ for MIL-101 without Cu
563 against 3420 $mg \cdot g^{-1}$ with Cu nanoparticles. Results obtained for MIL-101 without Cu are not
564 so far from the computational study done by Salles and Zajac where a capacity of around
565 2200 $mg \cdot g^{-1}$ was estimated under the same conditions [109]. Studies on organic iodide
566 trapping were also carried out with MIL-101 [110]. The dynamic test in presence of CH_3I/N_2
567 gas (done at 150 °C) indicated a capacity of around 240 $mg \cdot g^{-1}$. This result (rather low) could
568 be explained by the high temperature condition of the test or the larger volume of CH_3I
569 (compared to I_2). However, like for UiO-66, by modifying organic linkers, it is possible to
570 increase the capacity. With triethylenediamine and hexamethylenetetramine, capacities of 710
571 $mg \cdot g^{-1}$ and 620 $mg \cdot g^{-1}$ can be reached respectively. The authors explained this improvement
572 by a better stability of the modified MIL-100 against temperature.
573 MOF-808 was studied by Wang et al. in order to obtain bead-shaped sorbents of around 2 mm
574 of diameter [111]. This type of study is of interest in the perspective of an industrial use of
575 MOFs for iodine trapping where easy to handle materials are targeted. Their sorbents
576 (obtained through a wet synthesis by addition of poly(vinylidenefluoride) at 30 wt.%) can trap
577 1420 $mg \cdot g^{-1}$ of iodine in static conditions at 80 °C during 24 h. However, it is lower than the
578 powdery form of MOF-808 for which 2010 $mg \cdot g^{-1}$ was obtained. In dynamic conditions, the
579 same capacity was obtained (1360 $mg \cdot g^{-1}$) and the authors demonstrated that the time to reach
580 saturation was shorter when temperature and iodine concentration increased. On the other
581 hand, the presence of water makes these sorbents less efficient due to the hydrophilic property
582 of Zr metal in the structure.

583 Some unusual MOFs have also been studied for gaseous iodine trapping like NUC-5 with In
584 as metallic cluster [112]. I_2 capture test in static conditions at 77 °C indicated a capacity of
585 780 $mg \cdot g^{-1}$. However, thermogravimetric analysis highlighted an iodine release from 30 °C up
586 to 200 °C, temperature for which no more iodine was present. Modified MIF-53 with fumaric
587 acid demonstrated good iodine capture properties [113]. Tests performed under static
588 conditions at different temperatures (room temperature up to 70 °C) revealed a capacity of
589 around 1120 $mg \cdot g^{-1}$ for the test carried out at 70 °C. Gogia et al. synthetized a nitrogen-rich
590 3D MOF which has the particularity of trapping I_2 in static conditions at 70 °C with a capacity
591 of 2130 $mg \cdot g^{-1}$.
592 New types of MOFs allowing the trapping of iodine by chemisorption are also under
593 investigation. The aim is to obtain sorbents that can retain iodine at high temperature which
594 could be particularly useful in the case of a nuclear accident or if a heat-treatment is necessary
595 to obtain a conditioning matrix. Jung et al. developed a bismuth-based MOF (Bi-mna) which
596 can trap around 700 $mg \cdot g^{-1}$ of iodine in static conditions from 77 up to 300 °C [114]. Even if
597 its capacity is lower than that of other MOFs, none iodine release was measured out below
598 300 °C because of the formation of BiI_3 and Bi-O-I bonds.

599 ## 10. Conclusion and future prospects

600 This review has focused on the characteristics of solid sorbents for gaseous radioactive
601 iodine capture (I_2 or CH_3I), listed in Table 2, whose conversion into stable waste has been
602 described in the literature. The development of these materials has been guided by the
603 objective of producing a waste form suitable for deep geological storage to minimize their
604 radiological impact.
605 The sorbents can trap iodine by two different mechanisms. One is associated to physisorption
606 where iodine is weakly and reversible trapped on the surface thanks to Van der Waals-type

607 interactions. The other one using chemisorption insure an irreversible trapping of iodine
608 through the formation of strong chemical bonds between the active sites (metals, cations or
609 salts) and iodine. The active sites are often made of silver (Ag^0, Ag^+ or $AgNO_3$) because it has
610 an extremely strong thermodynamic affinity for iodine with correspondingly strong
611 interaction energies (less than -100 kJ·mol^{-1}). The reaction product of these reagents is AgI.
612 In some cases (minority report by comparison with silver), other metals like Bi or Cu are
613 considered.
614 The various silver-functionalized sorbents reviewed here, namely silver mordenites, silver-
615 silica aerogels and silver alumina can trap iodine efficiently at up to 200 mg·g^{-1}. In
616 chalcogels, other active sites such as Sb and Sn can be used, whereas in MOFs, the absence of
617 active sites means that iodine is exclusively trapped by physisorption in the pores of the
618 material. In this case, the pore size distribution can make the materials selective for certain
619 forms of iodine. Although physisorption is reversible, very high iodine loading capacities can
620 be achieved (> 1000 mg·g^{-1}). Note however that comparing the loading capacities in terms of
621 milligrams per gram of sorbent is difficult because the sorbents have different specific
622 masses. It would be more informative to express results in millimoles of iodine per mole of
623 sorbent, or as milligrams of iodine per cm^3 of sorbent.
624 To transform these sorbents into stable waste forms after iodine capture, the open porous
625 network has to be collapsed or blocked to limit the release of iodine in contact with a
626 propagation medium. This is achieved by heat treatment, in some cases at high pressure. HUP
627 and HIP have thereby been used to transform silver-functionalised sorbents directly, without
628 adjuvants. Results show that the waste forms obtained with HIP are less porous, with no
629 iodine release during the process. After both HUP and HIP, the solidified waste contains
630 multiple phases, with iodine present as AgI. Other types of sorbents can be vitrified. This
631 process is effective for lead bismuth sorbents, producing a homogeneous glass with no iodine

volatilisation. For chalcogels however, the release of vapours means the sorbents have to be vitrified in sealed quartz tubes. A multiphase material is obtained with iodine retained at the active sites. With MOFs finally, multiphase glass-composite waste forms with iodine trapped as AgI have been obtained by mixing the sorbent with glass powder and Ag^0, and then heat-treating pressed pellets of the mixture. Even though the iodine was initially physisorbed, none was released during the process, mainly thanks to the addition of Ag^0. Studies show that the volatility of iodine can be managed, but requires either a sealed environment, often with pressure treatment (such as in HIP), or low temperature vitrification, often with additional Ag^0 (to produce a homogenous glass or a composite in which the amorphous phase acts as a seal and diffusion barrier for the sorbent). The best choice of conversion process depends on the type of sorbent but also on technico-economic factors.

Very little data is available on the chemical durability of the waste forms produced, despite this being a crucial point in evaluating the radiological impact of these materials, since water is the main contact medium in geological storage. The data that are available were obtained under a variety of alteration conditions (H_2O or reducing environments, temperatures ranging from 25 to 90°C) and are difficult to extrapolate to the actual conditions in storage sites, which depend on the local geology, pH, groundwater composition, redox potential etc. Nevertheless, under anoxic conditions, thermodynamic data show that phases such as AgI are not stable and iodine trapped in this form is likely to be released [115,116]. It is therefore crucial to perform chemical durability tests in conditions that are representative of those in actual geological repositories.

Regarding immobilization matrices developed specifically for iodine with potentially high chemical durability [117–119], these are not compatible with current dry filtration systems for iodine capture. They may however serve as starting materials to synthesize new sorbents and provide a source of new solutions for effective iodine management.

Table 2. Summary of reviewed results.

	Silver-mordenite	Silver-silca aerogels	Silver alumina	Lead bismuth	Chalcogels	ZIF-8 and HKUST-1
Active sites	Ag^+ or Ag^0	Ag^+ or Ag^0	$AgNO_3$	$BiPbO_2NO_3$	1) S 2) Sb 3) Sn	None
Measured iodine sorption capacity	120 $mg \cdot g^{-1}$ with Ag^+ (dynamic test with CH_3I) 217 $mg \cdot g^{-1}$ with Ag^0 (dynamic test with CH_3I)	480 $mg \cdot g^{-1}$ (thiolated Ag^+, dynamic test with I_2) 517 $mg \cdot g^{-1}$ (unthiolated-Ag^+, static test with I_2) 555 $mg \cdot g^{-1}$ (unthiolated-Ag^0, static test with I_2)	- 230 $mg \cdot g^{-1}$ (dynamic test with CH_3I) - 220 $mg \cdot g^{-1}$ (dynamic test with I_2)	Not reported	1) 680 $mg \cdot g^{-1}$ (static test with I_2) 2) 540 $mg \cdot g^{-1}$ (static test with I_2) 3) 2250 $mg \cdot g^{-1}$ (static test with I_2)	- ZIF-8: 1250 $mg \cdot g^{-1}$ (static test with I_2) - ZIF-8: 7 $mg \cdot g^{-1}$ (dynamic test with CH_3I) - HKUST-1: 1750 $mg \cdot g^{-1}$ (static test with I_2) - HKUST-1: 1425 $mg \cdot g^{-1}$ (dynamic test with CH_3I)
Iodine capture mechanism	Chemisorption	Chemisorption	Chemisorption	Chemisorption	Chemisorption	Physisorption
Contaminants and sensitivities	- Hydrocarbons and CO for low Ag^+ content - NOx and H_2O for Ag^0	NO and H_2O for thiolated Ag^+ gel No information for unthiolated gels	H_2O for pores < 50 nm	Not reported	Not available	Not available
Conversion into stable waste forms	Starting from Ag^0 material: 1) HUP (750 °C, 27.5 MPa) 2) HIP (700 °C, 175 MPa) 3) HUP with addition of glass and Ag^0 flakes (550 °C, 70 MPa)	Starting from thiolated-Ag^+ gel: 1) HUP (1200 °C, 29 MPa) 2) HIP (1200 °C, 207 MPa)	HIP (1200 °C, 175 MPa)	Vitrification with ZnO (540 °C)	1) Vitrification in quartz tube with GeS_2 (600 °C) 2) Vitrification in quartz tube (600 °C) 3) Vitrification in quartz tube with Sb_2S_3 (600 °C)	Pressing followed by thermal treatment (500 °C): with Bi_2O_3-ZnO-B_2O_3 and Ag^0 1) I_2-loaded ZIF-8 2) I_2-loaded HKUST-1 with Bi_2O_3-ZnO-SIO_2 and Ag^0 3) I_2-loaded ZIF-8 4) I_2-loaded HKUST-1

Waste form microstructure	Only for Ag^0 material: 1) Not reported 2) Glass + AgI + $AgI(IO_4)$ 3) Glass + AgI + $Bi_4(SiO_4)_2$ + mordénite	Only for thiolated-Ag^+ gel: 1) Not reported 2) Glass + AgI + Ag^0 + Ag_2S	AgI + Al_2O_3	Homogeneous glass	1) Glass + SnI_4 + SiO_2 + GeS_4 2) SbSI, SbI_3, SiO_2 3) Glass + SbI_3 + SbSI	1) BiOI + BiI_3 + Ag^0 + AgI 2) BiOI + $Bi_{12}SiO_{20}$ + Ag^0 + AgI 3) Glass + Ag^0 + AgI 4) Glass + Ag^0 + AgI
Chemical durability	Only for Ag^0 material: 1) Not studied 2) Not studied 3) Deionized water at 90 °C for 7 d. Low release of glass elements	Not studied	Not studied	Reducing environment at 25 °C for 7 d. Formation of alteration layer limiting iodine release	Not studied	For all waste forms: Deionized water at 90 °C for 7 d. Negligible iodine release except for 1)

11. References

[1] M. Harrison, Vitrification of High Level Waste in the UK, Procedia Materials Science. 7 (2014). https://doi.org/10.1016/j.mspro.2014.10.003.

[2] A. Goel, J.S. McCloy, R. Pokorny, A.A. Kruger, Challenges with vitrification of Hanford High-Level Waste (HLW) to borosilicate glass – An overview, Journal of Non-Crystalline Solids: X. 4 (2019) 100033. https://doi.org/10.1016/j.nocx.2019.100033.

[3] J.D. Vienna, Nuclear Waste Vitrification in the United States: Recent Developments and Future Options, International Journal of Applied Glass Science. 1 (2010) 309–321. https://doi.org/10.1111/j.2041-1294.2010.00023.x.

[4] G. Roth, S. Weisenburger, Vitrification of high-level liquid waste: glass chemistry, process chemistry and process technology, Nuclear Engineering and Design. 202 (2000) 197–207. https://doi.org/10.1016/S0029-5493(00)00358-7.

[5] S. Yamashita, S. Suzuki, Risk of thyroid cancer after the Fukushima nuclear power plant accident, Respiratory Investigation. 51 (2013) 128–133. https://doi.org/10.1016/j.resinv.2013.05.007.

[6] F.N. von Hippel, The radiological and psychological consequences of the Fukushima Daiichi accident, Bulletin of the Atomic Scientists. 67 (2011) 27–36. https://doi.org/10.1177/0096340211421588.

[7] J.E.T. Hoeve, M. Z. Jacobson, Worldwide health effects of the Fukushima Daiichi nuclear accident, Energy & Environmental Science. 5 (2012) 8743–8757. https://doi.org/10.1039/C2EE22019A.

[8] X. Sun, Z. Shan, W. Teng, Effects of Increased Iodine Intake on Thyroid Disorders, Endocrinol Metab (Seoul). 29 (2014) 240–247. https://doi.org/10.3803/EnM.2014.29.3.240.

[9] S. Yamashita, S. Suzuki, S. Suzuki, H. Shimura, V. Saenko, Lessons from Fukushima: Latest Findings of Thyroid Cancer After the Fukushima Nuclear Power Plant Accident, Thyroid. 28 (2018) 11–22. https://doi.org/10.1089/thy.2017.0283.

[10] B.J. Riley, M.J. Schweiger, D.-S. Kim, W.W. Lukens, B.D. Williams, C. Iovin, C.P. Rodriguez, N.R. Overman, M.E. Bowden, D.R. Dixon, J.V. Crum, J.S. McCloy, A.A. Kruger, Iodine solubility in a low-activity waste borosilicate glass at 1000°C, Journal of Nuclear Materials. 452 (2014) 178–188. https://doi.org/10.1016/j.jnucmat.2014.04.027.

[11] V. Jolivet, Y. Morizet, M. Paris, T. Suzuki-Muresan, High pressure experimental study on iodine solution mechanisms in nuclear waste glasses, Journal of Nuclear Materials. 533 (2020) 152112. https://doi.org/10.1016/j.jnucmat.2020.152112.

[12] P.R. Hrma, Retention of Halogens in Waste Glass, Pacific Northwest National Lab. (PNNL), Richland, WA (United States), 2010. https://doi.org/10.2172/981571.

[13] J. Magill, H. Schwoerer, F. Ewald, J. Galy, R. Schenkel, R. Sauerbrey, Laser transmutation of iodine-129, Appl. Phys. B. 77 (2003) 387–390. https://doi.org/10.1007/s00340-003-1306-4.

[14] R.J.M. Konings, Transmutation of iodine: results of the EFTTRA-T1 irradiation test, Journal of Nuclear Materials. 244 (1997) 16–21. https://doi.org/10.1016/S0022-3115(96)00729-5.

[15] D. Li, K. Imasaki, K. Horikawa, S. Miyamoto, S. Amano, T. Mochizuki, Iodine Transmutation through Laser Compton Scattering Gamma Rays, Journal of Nuclear Science and Technology. 46 (2009) 831–835. https://doi.org/10.1080/18811248.2007.9711592.

[16] W.C. Wolkenhauer, J. Leonard, B.F. Gore, Transmutation of high-level radioactive waste with a controlled thermonuclear reactor, Battelle Pacific Northwest Labs., Richland, Wash. (USA), 1973. https://doi.org/10.2172/4407391.

[17] B.J. Riley, J.D. Vienna, D.M. Strachan, J.S. McCloy, J.L. Jerden, Materials and processes for the effective capture and immobilization of radioiodine: A review, Journal of Nuclear Materials. 470 (2016) 307–326. https://doi.org/10.1016/j.jnucmat.2015.11.038.

[18] C. Cao, A. Goel, Apatite based ceramic waste forms for immobilization of radioactive iodine – An overview, in: 2016. https://doi.org/10.13140/RG.2.2.11993.11362.

[19] A. Coulon, A. Grandjean, D. Laurencin, P. Jollivet, S. Rossignol, L. Campayo, Durability testing of an iodate-substituted hydroxyapatite designed for the conditioning of 129I, Journal of Nuclear Materials. 484 (2017) 324–331. https://doi.org/10.1016/j.jnucmat.2016.10.047.

[20] F. Audubert, J. Carpena, J.L. Lacout, F. Tetard, Elaboration of an iodine-bearing apatite Iodine diffusion into a Pb3(VO4)2 matrix, Solid State Ionics. 95 (1997) 113–119. https://doi.org/10.1016/S0167-2738(96)00570-X.

[21] J. Wang, Incorporation of iodine into apatite structure: a crystal chemistry approach using Artificial Neural Network, Frontiers in Earth Science. 3 (2015) 20. https://doi.org/10.3389/feart.2015.00020.

[22] F. Gauthier-Lafaye, P. Holliger, P.-L. Blanc, Natural fission reactors in the Franceville basin, Gabon: A review of the conditions and results of a “critical event” in a geologic system, Geochimica et Cosmochimica Acta. 60 (1996) 4831–4852. https://doi.org/10.1016/S0016-7037(96)00245-1.

[23] V. Sere, Geochemistry of neo-formed minerals at Oklo (Gabon), geologic history of the Oklo basin: a contribution for the studies of geologic disposals of radioactive wastes, France, 1996.

[24] A.-L. Chabauty, F.O. Méar, L. Montagne, L. Campayo, Chemical durability evaluation of silver phosphate–based glasses designed for the conditioning of radioactive iodine,

Journal of Nuclear Materials. 550 (2021) 152919. https://doi.org/10.1016/j.jnucmat.2021.152919.

[25] R. Pénélope, L. Campayo, M. Fournier, A. Gossard, A. Grandjean, Silver-phosphate glass matrix for iodine conditioning: from sorbent design to vitrification, Journal of Nuclear Materials. (2021) 153352. https://doi.org/10.1016/j.jnucmat.2021.153352.

[26] J.H. Yang, H.-S. Park, Y.-Z. Cho, Silver phosphate glasses for immobilization of radioactive iodine, Annals of Nuclear Energy. 110 (2017) 208–214. https://doi.org/10.1016/j.anucene.2017.06.042.

[27] H. Fujihara, T. Murase, T. Nisli, K. Noshita, T. Yoshida, M. Matsuda, Low Temperature Vitrification of Radioiodine Using AgI-Ag2O-P2O5 Glass System, MRS Online Proceedings Library (OPL). 556 (1999). https://doi.org/10.1557/PROC-556-375.

[28] Daryl Haefner, Methods of Gas Phase Capture of Iodine from Fuel Reprocessing Off-Gas: A Literature Survey, 2007. https://doi.org/10.2172/911962.

[29] R.T. Jubin, Airborne waste management technology applicable for use in reprocessing plants for control of iodine and other off-gas constituents, Oak Ridge National Lab., TN (USA), 1988. https://doi.org/10.2172/5169490.

[30] L.L. Burger, R.D. Scheele, PNNL-14860 HWVP Iodine Trap Evaluation, 2004.

[31] D.E. Horner, J.C. Mailen, F.A. Posey, Electrolytic trapping of iodine from process gas streams, US4004993A, 1977. https://patents.google.com/patent/US4004993/en (accessed November 12, 2020).

[32] P. Paviet-Hartmann, W. Kerlin, S. Bakhtiar, TREATMENT OF GASEOUS EFFLUENTS ISSUED FROM RECYCLING – A REVIEW OF THE CURRENT PRACTICES AND PROSPECTIVE IMPROVEMENTS, (n.d.) 12.

[33] J. Huve, A. Ryzhikov, H. Nouali, V. Lalia, G. Augé, T.J. Daou, Porous sorbents for the capture of radioactive iodine compounds: a review, RSC Adv. 8 (2018) 29248–29273. https://doi.org/10.1039/C8RA04775H.

[34] S.U. Nandanwar, K. Coldsnow, V. Utgikar, P. Sabharwall, D. Eric Aston, Capture of harmful radioactive contaminants from off-gas stream using porous solid sorbents for clean environment – A review, Chemical Engineering Journal. 306 (2016) 369–381. https://doi.org/10.1016/j.cej.2016.07.073.

[35] W. Xie, D. Cui, S.-R. Zhang, Y.-H. Xu, D.-L. Jiang, Iodine capture in porous organic polymers and metal–organic frameworks materials, Mater. Horiz. 6 (2019) 1571–1595. https://doi.org/10.1039/C8MH01656A.

[36] D.F. Sava, K.W. Chapman, M.A. Rodriguez, J.A. Greathouse, P.S. Crozier, H. Zhao, P.J. Chupas, T.M. Nenoff, Competitive I2 Sorption by Cu-BTC from Humid Gas Streams, Chem. Mater. 25 (2013) 2591–2596. https://doi.org/10.1021/cm401762g.

[37] D. Banerjee, X. Chen, S.S. Lobanov, A.M. Plonka, X. Chan, J.A. Daly, T. Kim, P.K. Thallapally, J.B. Parise, Iodine Adsorption in Metal Organic Frameworks in the Presence of Humidity, ACS Appl. Mater. Interfaces. 10 (2018) 10622–10626. https://doi.org/10.1021/acsami.8b02651.

[38] G. Massasso, J. Long, J. Haines, S. Devautour-Vinot, G. Maurin, A. Grandjean, B. Onida, B. Donnadieu, J. Larionova, C. Guérin, Y. Guari, Iodine Capture by Hofmann-Type Clathrate NiII(pz)[NiII(CN)4], Inorg. Chem. 53 (2014) 4269–4271. https://doi.org/10.1021/ic500048z.

[39] H. Sun, B. Yang, A. Li, Biomass derived porous carbon for efficient capture of carbon dioxide, organic contaminants and volatile iodine with exceptionally high uptake, Chemical Engineering Journal. 372 (2019) 65–73. https://doi.org/10.1016/j.cej.2019.04.061.

[40] H. Sun, P. La, R. Yang, Z. Zhu, W. Liang, B. Yang, A. Li, W. Deng, Innovative nanoporous carbons with ultrahigh uptakes for capture and reversible storage of CO2 and volatile iodine, Journal of Hazardous Materials. 321 (2017) 210–217. https://doi.org/10.1016/j.jhazmat.2016.09.015.

[41] H. Sun, P. La, Z. Zhu, W. Liang, B. Yang, A. Li, Capture and reversible storage of volatile iodine by porous carbon with high capacity, J Mater Sci. 50 (2015) 7326–7332. https://doi.org/10.1007/s10853-015-9289-1.

[42] F. Rouquerol, J. Rouquerol, K. Sing, CHAPTER 11 - Adsorption by Clays, Pillared Layer Structures and Zeolites, in: F. Rouquerol, J. Rouquerol, K. Sing (Eds.), Adsorption by Powders and Porous Solids, Academic Press, London, 1999: pp. 355–399. https://doi.org/10.1016/B978-012598920-6/50012-9.

[43] M.M. Mohamed, T.M. Salama, I. Othman, I.A. Ellah, Synthesis of high silica mordenite nanocrystals using o-phenylenediamine template, Microporous and Mesoporous Materials. 84 (2005) 84–96. https://doi.org/10.1016/j.micromeso.2005.05.017.

[44] M.B.Z. Gili, M.T. Conato, Synthesis and characterization of mordenite-type zeolites with varying Si/Al ratio, Mater. Res. Express. 6 (2018) 015515. https://doi.org/10.1088/2053-1591/aae8db.

[45] S. Chibani, M. Chebbi, S. Lebègue, L. Cantrel, M. Badawi, Impact of the Si/Al ratio on the selective capture of iodine compounds in silver-mordenite: a periodic DFT study, Phys. Chem. Chem. Phys. 18 (2016) 25574–25581. https://doi.org/10.1039/C6CP05015H.

[46] H. Zhao, T.M. Nenoff, G. Jennings, P.J. Chupas, K.W. Chapman, Determining Quantitative Kinetics and the Structural Mechanism for Particle Growth in Porous Templates, J. Phys. Chem. Lett. 2 (2011) 2742–2746. https://doi.org/10.1021/jz201260n.

[47] Y. Nan, L.L. Tavlarides, D.W. DePaoli, Adsorption of iodine on hydrogen-reduced silver-exchanged mordenite: Experiments and modeling, AIChE Journal. (2016). https://doi.org/10.1002/aic.15432.

[48] R.D. Scheele, L.L. Burger, C.L. Matsuzaki, Methyl Iodide Sorption by Reduced Silver Mordenite, (1983).

[49] M. Chebbi, S. Chibani, J.-F. Paul, L. Cantrel, M. Badawi, Evaluation of volatile iodine trapping in presence of contaminants: A periodic DFT study on cation exchanged-faujasite, Microporous and Mesoporous Materials. 239 (2017) 111–122. https://doi.org/10.1016/j.micromeso.2016.09.047.

[50] H. Jabraoui, E.P. Hessou, S. Chibani, L. Cantrel, S. Lebègue, M. Badawi, Adsorption of volatile organic and iodine compounds over silver-exchanged mordenites: A comparative periodic DFT study for several silver loadings, Applied Surface Science. 485 (2019) 56–63. https://doi.org/10.1016/j.apsusc.2019.03.282.

[51] B. Azambre, M. Chebbi, Evaluation of Silver Zeolites Sorbents Toward Their Ability to Promote Stable CH3I Storage as AgI Precipitates, ACS Appl. Mater. Interfaces. 9 (2017) 25194–25203. https://doi.org/10.1021/acsami.7b02366.

[52] T.M. Nenoff, M.A. Rodriguez, N.R. Soelberg, K.W. Chapman, Silver-mordenite for radiologic gas capture from complex streams: Dual catalytic CH3I decomposition and I confinement, Microporous and Mesoporous Materials. 200 (2014) 297–303. https://doi.org/10.1016/j.micromeso.2014.04.041.

[53] K.W. Chapman, P.J. Chupas, T.M. Nenoff, Radioactive Iodine Capture in Silver-Containing Mordenites through Nanoscale Silver Iodide Formation, J. Am. Chem. Soc. 132 (2010) 8897–8899. https://doi.org/10.1021/ja103110y.

[54] R. Jubin, S. Bruffey, K. Patton, Expanded Analysis of Hot Isostatic Pressed Iodine-Loaded Silver-Exchanged Mordenite, 2014. https://doi.org/10.2172/1160345.

[55] T.J. Garino, T.M. Nenoff, D.F. Sava Gallis, Densified waste form and method for forming, Sandia National Lab. (SNL-NM), Albuquerque, NM (United States), 2016. https://www.osti.gov/doepatents/biblio/1253342-densified-waste-form-method-forming (accessed October 20, 2021).

[56] T.J. Garino, T.M. Nenoff, J.L. Krumhansl, D.X. Rademacher, Low-Temperature Sintering Bi–Si–Zn-Oxide Glasses for Use in Either Glass Composite Materials or Core/Shell 129I Waste Forms, Journal of the American Ceramic Society. 94 (2011) 2412–2419. https://doi.org/10.1111/j.1551-2916.2011.04542.x.

[57] R. Jubin, S.H. Bruffey, High-Temperature Pressing of Silver-Exchanged Mordenite into a Potential Iodine Waste Form - 14096, Undefined. (2014). /paper/High-Temperature-Pressing-of-Silver-Exchanged-into-Jubin-Bruffey/0a3bcf598b345d4d598d8563fc8b7634f88eb917 (accessed December 1, 2020).

[58] M. Chebbi, B. Azambre, L. Cantrel, A. Koch, A Combined DRIFTS and DR-UV–Vis Spectroscopic In Situ Study on the Trapping of CH3I by Silver-Exchanged Faujasite Zeolite, J. Phys. Chem. C. 120 (2016) 18694–18706. https://doi.org/10.1021/acs.jpcc.6b07112.

[59] B. Azambre, M. Chebbi, A. Hijazi, Effects of the cation and Si/Al ratio on CH3I adsorption by faujasite zeolites, Chemical Engineering Journal. 379 (2020) 122308. https://doi.org/10.1016/j.cej.2019.122308.

[60] B.S. Choi, G.I. Park, J.H. Kim, J.W. Lee, S.K. Ryu, Adsorption Equilibrium and Dynamics of Methyl Iodide in a Silver Ion-Exchanged Zeolite Column at High Temperatures, Adsorption. 7 (2001) 91–103. https://doi.org/10.1023/A:1011660121182.

[61] M. Chebbi, B. Azambre, C. Monsanglant-Louvet, B. Marcillaud, A. Roynette, L. Cantrel, Effects of water vapour and temperature on the retention of radiotoxic CH3I by

silver faujasite zeolites, Journal of Hazardous Materials. 409 (2021) 124947. https://doi.org/10.1016/j.jhazmat.2020.124947.

[62] I. Smirnova, P. Gurikov, Aerogel production: Current status, research directions, and future opportunities, The Journal of Supercritical Fluids. 134 (2018) 228–233. https://doi.org/10.1016/j.supflu.2017.12.037.

[63] A.C. Pierre, G.M. Pajonk, Chemistry of Aerogels and Their Applications, Chem. Rev. 102 (2002) 4243–4266. https://doi.org/10.1021/cr0101306.

[64] Summary Report on the Volatile Radionuclide and Immobilization Research for FY2011 at PNNL | PNNL, (n.d.). https://www.pnnl.gov/publications/summary-report-volatile-radionuclide-and-immobilization-research-fy2011-pnnl (accessed December 14, 2020).

[65] S.H. Bruffey, R.T. Jubin, K.K. Anderson, J. Walker, AGING AND IODINE LOADING OF SILVER-FUNCTIONALIZED AEROGELS, Oak Ridge National Lab. (ORNL), Oak Ridge, TN (United States), 2013. https://www.osti.gov/biblio/1096292 (accessed December 14, 2020).

[66] S.H. Bruffey, K. Patton, R.T. Jubin, Complete Iodine Loading of NO-Aged Ag0-Functionalized Silica Aerogel, (2015).

[67] J. Matyáš, E.S. Ilton, L. Kovařík, Silver-functionalized silica aerogel: towards an understanding of aging on iodine sorption performance, RSC Adv. 8 (2018) 31843–31852. https://doi.org/10.1039/C8RA05137B.

[68] B.J. Riley, J.O. Kroll, J.A. Peterson, J. Matyáš, M.J. Olszta, X. Li, J.D. Vienna, Silver-Loaded Aluminosilicate Aerogels As Iodine Sorbents, ACS Appl. Mater. Interfaces. 9 (2017) 32907–32919. https://doi.org/10.1021/acsami.7b10290.

[69] J. Matyáš, N. Canfield, S. Sulaiman, M. Zumhoff, Silica-based waste form for immobilization of iodine from reprocessing plant off-gas streams, Journal of Nuclear Materials. 476 (2016) 255–261. https://doi.org/10.1016/j.jnucmat.2016.04.047.

[70] J. G. Wilhelm, Removal of Gaseous Radioiodine with Solid Adsorbents, INTERNATIONAL ATOMIC ENERGY AGENCY. (1982).

[71] F. J. Herrmann, Control of Radio-Iodine at the German Reprocessing Plant WAK during Operation and after Shutdown, Proceedings of the 24th DOE/NRC Nuclear Air Cleaning and Treatment Conference, United-States, 1997.

[72] J. G. Wilhelm, Head-end Iodine Removal From a Reprocessing Plant With a Solide Sorbent, Proceedings of the 14th ERDA Air Cleaning Conference, United-States, 1977.

[73] R. Wada, T. Nishimura, O. Kato, Y. Kurimoto, T. Imakita, T. Kozawa, N. Saito, H. Fujihara, Manufacturing of rock solidified waste by HIP, Nippon Genshiryoku Gakkai Wabun Ronbunshi. 3 (2004). https://www.osti.gov/etdeweb/biblio/20488375 (accessed March 30, 2021).

[74] T. Fukasawa, Influences of Impurities on Iodine Removal Efficiency of Silver Alumina Adsorbent, Proceedings of the 24th DOE/NRC Nuclear Air Cleaning and Treatment Conference, United-States, 1997.

[75] T. FUKASAWA, K. FUNABASHI, Y. KONDO, Separation Technology for Radioactive Iodine from Off-Gas Streams of Nuclear Facilities, Journal of Nuclear Science and Technology. 31 (1994) 1073–1083. https://doi.org/10.1080/18811248.1994.9735261.

[76] 程庆辉李泽军, L.Z.-J. CHENG Qing-Hui, Adsorption of gaseous iodine-131 at high temperatures by silver impregnated alumina, 《核技术》(英文版) ISSN 1001-8042 CN 31-1559/TL. 26 (2015) 40303–040303. https://doi.org/10.13538/j.1001-8042/nst.26.040303.

[77] M. Kikuchi, M. Kitamura, H. Yusa, S. Horiuchi, Removal of radioactive methyl iodide by silver impregnated alumina and zeolite, Nuclear Engineering and Design. 47 (1978) 283–287. https://doi.org/10.1016/0029-5493(78)90071-7.

[78] K. Funabashi, T. Fukasawa, M. Kikuchi, Investigation of Silver-Impregnated Alumina for Removal of Radioactive Methyl Iodide, Nuclear Technology. 109 (1995) 366–372. https://doi.org/10.13182/NT95-A35085.

[79] K. Masuda, O. Kato, Y. Tanaka, S. Nakajima, S. Okamoto, T. Sakuragi, S. Yoshida, Iodine immobilization: Development of solidification process for spent silver-sorbent using hot isostatic press technique, Progress in Nuclear Energy. 92 (2016) 267–272. https://doi.org/10.1016/j.pnucene.2015.09.012.

[80] A. Mukunoki, T. Chiba, Y. Suzuki, K. Yamaguchi, T. Sakuragi, T. Nanba, Further Development of Iodine Immobilization Technique by Low Temperature Vitrification With BiPbO2I, in: American Society of Mechanical Engineers Digital Collection, 2010: pp. 329–334. https://doi.org/10.1115/ICEM2009-16268.

[81] B.J. Riley, D.A. Pierce, J. Chun, Efforts to Consolidate Chalcogels with Adsorbed Iodine, UNT Digital Library. (2013). https://doi.org/10.2172/1097940.

[82] K.S. Subrahmanyam, D. Sarma, C.D. Malliakas, K. Polychronopoulou, B.J. Riley, D.A. Pierce, J. Chun, M.G. Kanatzidis, Chalcogenide Aerogels as Sorbents for Radioactive Iodine, Chem. Mater. 27 (2015) 2619–2626. https://doi.org/10.1021/acs.chemmater.5b00413.

[83] D. Ruffolo, P. Boolchand, Origin of glass formation, Phys. Rev. Lett. 55 (1985) 242–245. https://doi.org/10.1103/PhysRevLett.55.242.

[84] B.J. Riley, W.C. Lepry, Initial Assessment of the Consolidation of Chalcogels into a Viable Waste Form, Pacific Northwest National Lab. (PNNL), Richland, WA (United States), 2012. https://doi.org/10.2172/1051204.

[85] D. Savytskii, B. Knorr, V. Dierolf, H. Jain, Laser-induced growth of oriented Sb2S3 single crystal dots on the surface of 82SbSI–18Sb2S3 glasses, Journal of Non-Crystalline Solids. 431 (2016) 36–40. https://doi.org/10.1016/j.jnoncrysol.2015.03.007.

[86] E. Drioli, L. Giorno, eds., Encyclopedia of Membranes, Springer-Verlag, Berlin Heidelberg, 2016. https://www.springer.com/gp/book/9783662443231 (accessed November 16, 2020).

[87] S.D. Worrall, M.A. Bissett, P.I. Hill, A.P. Rooney, S.J. Haigh, M.P. Attfield, R.A.W. Dryfe, Metal-organic framework templated electrodeposition of functional gold nanostructures, Electrochimica Acta. 222 (2016) 361–369. https://doi.org/10.1016/j.electacta.2016.10.187.

[88] D.F. Sava, M.A. Rodriguez, K.W. Chapman, P.J. Chupas, J.A. Greathouse, P.S. Crozier, T.M. Nenoff, Capture of Volatile Iodine, a Gaseous Fission Product, by Zeolitic Imidazolate Framework-8, J. Am. Chem. Soc. 133 (2011) 12398–12401. https://doi.org/10.1021/ja204757x.

[89] K.W. Chapman, D.F. Sava, G.J. Halder, P.J. Chupas, T.M. Nenoff, Trapping Guests within a Nanoporous Metal–Organic Framework through Pressure-Induced Amorphization, J. Am. Chem. Soc. 133 (2011) 18583–18585. https://doi.org/10.1021/ja2085096.

[90] Y. Yuan, X. Dong, Y. Chen, M. Zhang, Computational screening of iodine uptake in zeolitic imidazolate frameworks in a water-containing system, Phys. Chem. Chem. Phys. 18 (2016) 23246–23256. https://doi.org/10.1039/C6CP02156E.

[91] D.F. Sava Gallis, I. Ermanoski, J.A. Greathouse, K.W. Chapman, T.M. Nenoff, Iodine Gas Adsorption in Nanoporous Materials: A Combined Experiment–Modeling Study, Ind. Eng. Chem. Res. 56 (2017) 2331–2338. https://doi.org/10.1021/acs.iecr.6b04189.

[92] P.-H. Tang, P.B. So, K.-R. Lee, Y.-L. Lai, C.-S. Lee, C.-H. Lin, Metal Organic Framework-Polyethersulfone Composite Membrane for Iodine Capture, Polymers. 12 (2020) 2309. https://doi.org/10.3390/polym12102309.

[93] D.F. Sava, M.A. Rodriguez, K.W. Chapman, P.J. Chupas, J.A. Greathouse, P.S. Crozier, T.M. Nenoff, Capture of Volatile Iodine, a Gaseous Fission Product, by Zeolitic Imidazolate Framework-8, J. Am. Chem. Soc. 133 (2011) 12398–12401. https://doi.org/10.1021/ja204757x.

[94] M. Chebbi, B. Azambre, C. Volkringer, T. Loiseau, Dynamic sorption properties of Metal-Organic Frameworks for the capture of methyl iodide, Microporous and Mesoporous Materials. 259 (2018) 244–254. https://doi.org/10.1016/j.micromeso.2017.10.018.

[95] J.B. James, Y.S. Lin, Kinetics of ZIF-8 Thermal Decomposition in Inert, Oxidizing, and Reducing Environments, J. Phys. Chem. C. 120 (2016) 14015–14026. https://doi.org/10.1021/acs.jpcc.6b01208.

[96] J.T. Hughes, D.F. Sava, T.M. Nenoff, A. Navrotsky, Thermochemical Evidence for Strong Iodine Chemisorption by ZIF-8, J. Am. Chem. Soc. 135 (2013) 16256–16259. https://doi.org/10.1021/ja406081r.

[97] T.D. Bennett, P.J. Saines, D.A. Keen, J.-C. Tan, A.K. Cheetham, Ball-Milling-Induced Amorphization of Zeolitic Imidazolate Frameworks (ZIFs) for the Irreversible Trapping of Iodine, Chemistry – A European Journal. 19 (2013) 7049–7055. https://doi.org/10.1002/chem.201300216.

[98] L.J. Small, R.C. Hill, J.L. Krumhansl, M.E. Schindelholz, Z. Chen, K.W. Chapman, X. Zhang, S. Yang, M. Schröder, T.M. Nenoff, Reversible MOF-Based Sensors for the Electrical Detection of Iodine Gas, ACS Appl. Mater. Interfaces. 11 (2019) 27982–27988. https://doi.org/10.1021/acsami.9b09938.

[99] L.J. Small, J.L. Krumhansl, D.X. Rademacher, T.M. Nenoff, Iodine detection in Ag-mordenite based sensors: Charge conduction pathway determinations, Microporous and

Mesoporous Materials. 280 (2019) 82–87. https://doi.org/10.1016/j.micromeso.2019.01.051.

[100] L.J. Small, T.M. Nenoff, Direct Electrical Detection of Iodine Gas by a Novel Metal–Organic-Framework-Based Sensor, ACS Appl. Mater. Interfaces. 9 (2017) 44649–44655. https://doi.org/10.1021/acsami.7b16381.

[101] D.F. Sava, T.J. Garino, T.M. Nenoff, Iodine Confinement into Metal–Organic Frameworks (MOFs): Low-Temperature Sintering Glasses To Form Novel Glass Composite Material (GCM) Alternative Waste Forms, Ind. Eng. Chem. Res. 51 (2012) 614–620. https://doi.org/10.1021/ie200248g.

[102] P.D. Editor Robert C. Weast, CRC Handbook of Chemistry & Physics 59th Edition 1978-1979, n.d.

[103] P. Chen, X. He, M. Pang, X. Dong, S. Zhao, W. Zhang, Iodine Capture Using Zr-Based Metal–Organic Frameworks (Zr-MOFs): Adsorption Performance and Mechanism, ACS Appl. Mater. Interfaces. 12 (2020) 20429–20439. https://doi.org/10.1021/acsami.0c02129.

[104] M. Zahid, D. Zhang, X. Xu, M. Pan, M.H. ul haq, A.T. Reda, W. Xu, Barbituric and thiobarbituric acid-based UiO-66-NH2 adsorbents for iodine gas capture: Characterization, efficiency and mechanisms, Journal of Hazardous Materials. 416 (2021) 125835. https://doi.org/10.1016/j.jhazmat.2021.125835.

[105] Z.-J. Li, Y. Ju, H. Lu, X. Wu, X. Yu, Y. Li, X. Wu, Z.-H. Zhang, J. Lin, Y. Qian, M.-Y. He, J.-Q. Wang, Boosting the Iodine Adsorption and Radioresistance of Th-UiO-66 MOFs via Aromatic Substitution, Chemistry – A European Journal. 27 (2021) 1286–1291. https://doi.org/10.1002/chem.202003621.

[106] J. Maddock, X. Kang, L. Liu, B. Han, S. Yang, M. Schröder, The Impact of Structural Defects on Iodine Adsorption in UiO-66, Chemistry. 3 (2021) 525–531. https://doi.org/10.3390/chemistry3020037.

[107] M. Leloire, J. Dhainaut, P. Devaux, O. Leroy, H. Desjonqueres, S. Poirier, P. Nerisson, L. Cantrel, S. Royer, T. Loiseau, C. Volkringer, Stability and radioactive gaseous iodine-131 retention capacity of binderless UiO-66-NH2 granules under severe nuclear accidental conditions, Journal of Hazardous Materials. 416 (2021) 125890. https://doi.org/10.1016/j.jhazmat.2021.125890.

[108] B. Qi, Y. Liu, T. Zheng, Q. Gao, X. Yan, Y. Jiao, Y. Yang, Highly efficient capture of iodine by Cu/MIL-101, Journal of Solid State Chemistry. 258 (2018) 49–55. https://doi.org/10.1016/j.jssc.2017.09.031.

[109] F. Salles, J. Zajac, Impact of Structural Functionalization, Pore Size, and Presence of Extra-Framework Ions on the Capture of Gaseous I2 by MOF Materials, Nanomaterials. 11 (2021) 2245. https://doi.org/10.3390/nano11092245.

[110] B. Li, X. Dong, H. Wang, D. Ma, K. Tan, S. Jensen, B.J. Deibert, J. Butler, J. Cure, Z. Shi, T. Thonhauser, Y.J. Chabal, Y. Han, J. Li, Capture of organic iodides from nuclear waste by metal-organic framework-based molecular traps, Nat Commun. 8 (2017) 485. https://doi.org/10.1038/s41467-017-00526-3.

[111] L. Wang, P. Chen, X. Dong, W. Zhang, S. Zhao, S. Xiao, Y. Ouyang, Porous MOF-808@PVDF beads for removal of iodine from gas streams, RSC Adv. 10 (2020) 44679–44687. https://doi.org/10.1039/D0RA08741F.

[112] H. Chen, L. Fan, X. Zhang, L. Ma, Nanocage-Based InIII{TbIII}2-Organic Framework Featuring Lotus-Shaped Channels for Highly Efficient CO2 Fixation and I2 Capture, ACS Appl Mater Interfaces. 12 (2020) 27803–27811. https://doi.org/10.1021/acsami.0c07061.

[113] X. Chen, X. Jiang, X. Lei, B. Zhang, M. Qiao, C. Yin, Q. Zhang, Direct Synthesis of Two-Dimensional Metal–Organic Framework Nanoplates for Noble Metal Load and Gaseous Iodine Adsorption, Crystal Growth & Design. 20 (2020) 1378–1382. https://doi.org/10.1021/acs.cgd.9b01545.

[114] Y.-E. Jung, S.-W. Kang, M.-S. Yim, Feasibility Study of Using Bi-mna Metal–Organic Frameworks as Adsorbents for Radioiodine Capture at High Temperature, Ind. Eng. Chem. Res. 60 (2021) 5964–5975. https://doi.org/10.1021/acs.iecr.1c00450.

[115] T. Nishimura, T. Sakuragi, Y. Nasu, H. Asano, H. Tanabe, Development of immobilisation techniques for radioactive iodine for geological disposal, (2009). https://www.osti.gov/etdeweb/biblio/21251816 (accessed March 22, 2021).

[116] H. Tanabe, T. Sakuragi, K. Yamaguchi, T. Sato, H. Owada, Development of New Waste Forms to Immobilize Iodine-129 Released from a Spent Fuel Reprocessing Plant, Advances in Science and Technology. (2010). https://doi.org/10.4028/www.scientific.net/AST.73.158.

[117] A. Coulon, D. Laurencin, A. Grandjean, C.C.D. Coumes, S. Rossignol, L. Campayo, Immobilization of iodine into a hydroxyapatite structure prepared by cementation, J. Mater. Chem. A. 2 (2014) 20923–20932. https://doi.org/10.1039/C4TA03236E.

[118] C. Cao, S. Chong, L. Thirion, J.C. Mauro, J.S. McCloy, A. Goel, Wet chemical synthesis of apatite-based waste forms – A novel room temperature method for the immobilization of radioactive iodine, J. Mater. Chem. A. 5 (2017) 14331–14342. https://doi.org/10.1039/C7TA00230K.

[119] R.C. Moore, C.I. Pearce, J.W. Morad, S. Chatterjee, T.G. Levitskaia, R.M. Asmussen, A.R. Lawter, J.J. Neeway, N.P. Qafoku, M.J. Rigali, S.A. Saslow, J.E. Szecsody, P.K. Thallapally, G. Wang, V.L. Freedman, Iodine immobilization by materials through

sorption and redox-driven processes: A literature review, Science of The Total Environment. 716 (2020) 132820. https://doi.org/10.1016/j.scitotenv.2019.06.166.

Solid sorbents for gaseous iodine capture and their conversion into stable waste forms

R. Pénélope[1], L. Campayo[1], M. Fournier[1], A. Gossard[2], A. Grandjean[2]

[1] CEA, DES, ISEC, DE2D, University of Montpellier, Marcoule, Bagnols sur Cèze, France

[2] CEA, DES, ISEC, DMRC, University of Montpellier, Marcoule, Bagnols sur Cèze, France

raphael.penelope@cea.fr

CEA Marcoule, ISEC/DE2D/SEVT, Bât. 208, BP17171, 30207 Bagnols-sur-Cèze Cedex, France

Graphical abstract